Iraqi Journal of Physics, 2024 *Vol. 22, No. 2, PP. 104-115*
https://doi.org/10.30723/ijp.v22i2.1273 *P-ISSN: 2070-4003*
E-ISSN: 2664-5548

A Study the Addition of Silver Dioxide on Some Optical Properties of Phosphate Bioactive Glass

Ruqaya H. Hassan[1a*] and Dunia Kamil Mahdi[1b]
[1]*Department of Physics, College of Science, University of Baghdad, Baghdad, Iraq*
[b]E-mail: dunia.mahdi@sc.uobaghdad.edu.iq
[a*]Corresponding author: ruqaya.hassan1996@gmail.com

Abstract

This study investigates the influence of silver oxide (Ag_2O) concentration on the optical characteristics of phosphate bioactive glasses (PBGs). PBGs have emerged as promising alternatives to conventional silicate glasses in the medical field due to their excellent bioactivity and chemical resistance. Samples with varying Ag_2O concentrations (0, 0.25, 0.5, and 0.75g) were sintered at 780°C for 2 hrs in an electric furnace. The samples were subjected to Fourier transfer infrared spectroscopy (FTIR), ultraviolet-visible (UV-Vis) spectroscopy, and photoluminescence (PL) tests to assess their functional groups and optical properties. By analyzing the FTIR spectrum of phosphate bioactive glass containing different amounts of Ag_2O, it is possible to identify changes in the vibrational modes associated with Ag-O bonds and to gain insights into the structure and composition of the material. Because Ag-O bonds exhibit infrared vibrational modes, introducing Ag_2O changed the FTIR spectrum. As Ag_2O concentration increased, Ag-O vibrational modes strengthened, indicating more Ag-O bonds. UV-Vis spectroscopy, with increasing Ag_2O concentration, the peak location shifted towards shorter wavelengths. Optical spectra show distinct UV absorption in the prepared glass spectrum, extending to near visible with increasing Ag_2O content. The PL spectra peaks and band gap energies revealed that Ag_2O altered the glass's electrical structure and optical activity. These discoveries help optimize metal-phosphate bi-active glass for biomedical implants and UV-blocking coatings. The melting-annealing technique prepared glasses based on the base host Na_2O-CaF_2-P_2O_5 system with increasing Ag_2O as additives or loading (0.2 to 1 wt%).

Article Info.

Keywords:
Phosphate Bioactive Glass (PBG), Silicate Glasses, Calcium Di-Phosphate, Fourier-Transform Infrared Spectroscopy (FTIR), Strontium Carbonate ($SrCO_3$).

Article history:
Received: Jul. 10, 2023
Revised: Jan. 17, 2024
Accepted: Jan. 23, 2024
Published: Jun. 01,2024

1. Introduction

Phosphate bioactive glasses (PBGs) are a promising alternative to conventional silicate glasses for bone repair and reconstruction due to their adjustable chemical resistance that can be customized to meet specific application requirements [1-4]. Bioactive glasses (BGs) are attractive materials for tissue regeneration because of their biocompatibility and angiogenic and osteogenic characteristics [5, 6]. PBGs can be designed to degrade completely in a timeframe ranging from hours to years, making them an attractive material option [7]. They are produced by the melt-quenching technique, which requires the melting of precursor oxide powder at elevated temperatures (above 1000°C) followed by rapid cooling (quenching) of the melt to obtain an amorphous (non-crystalline) glass [8-10]. Glass-ceramic and surface-reactive materials based on biomaterials may be classified as bioactive glass [11]. This surface bioreactivity enables strong bonding with the surrounding bone tissue, which gives bioactive glasses (BGs) their osteon-conductive properties. Following their lease of dissolution products, BGs are also osteon inductive [12].

Abou Neel et al. [13] gave a general description of phosphate glasses, highlighting

their differences with their silicate based counterparts and explored what these glasses can offer in terms of biomedical applications. Particular focus was placed on phosphate glass chemistry, terminology and structure. The article concluded with a discussion of the future of phosphate-based glasses as biomaterials and highlighted possible avenues for potential applications. However, phosphate glasses are preferred in other applications, such as the release of oligoelements in soils. Moreover, the solubility of phosphate species in bio glass is responsible for the nucleation and apatite layer formation that is considered to be the main factor responsible for the bioactivity of bio glass.

BGs can be doped with silver (Ag) to boost their antibacterial activity. Using antibacterial materials can reduce the infection risk in order to reduce or eliminate the bacterial resistance problem [14]. Antibacterial metal ions have been around for a long time, and Ag has been shown to have good broad-spectrum bactericidal activity [15]. Ag-doped mesoporous bioactive glass (MBG) can be prepared by spray pyrolysis (SP) process to make a nanolayer of silver material on the surface of the MBG.

Incorporating metal ions, such as Ag, copper (Cu), or cobalt (Co), into glass compositions can modify their physical and chemical properties and provide unique functionality for clinical applications. Adding these metal ions can expand the potential applications of glasses in the biomedical field and improve their functionality [16]. Silver ions are highly effective against various microorganisms, including bacteria, viruses, and fungi, by disrupting their cellular processes [17, 18]. Doping phosphate-based glasses with copper ions has shown to enhance the bioactivity and antibacterial efficacy of the glass material against Staphylococcus aureus and Escherichia coli bacterial strains [19].

Due to its multivalent nature, silver may combine with oxygen to produce a variety of oxides, including AgO, Ag_2O, Ag_2O_3, and Ag_3O_4. However, based on currently available research, it has been determined that from all the above-mentioned silver oxides, AgO and Ag_2O have the most technologically significant uses and are also the easiest to make in laboratory settings [20, 21]. Traditional silicate bioactive glasses, according to studies, have crystallization kinetics that reduce the glass bioactivity while also impeding shape at medium to high temperatures [22, 23].

The biological activity of metallic ions introduced into BGs can aid hard and soft tissue repair therapy. These metallic ions are introduced into the BG network for a variety of reasons, including affecting the structure and process ability of the glass and imparting additional useful qualities [24]. Copper ions can damage the cell membranes of microorganisms, while cobalt ions not only have antibacterial properties but can also promote bone growth and enhance the mechanical strength of the glass [25]. Other well-known biologically active ions, such as strontium (Sr), boron (B), lithium and (Li), have also been incorporated in BGs to provide osteogenic, angiogenic, anti-inflammatory, and antibacterial effects. Rare earth and other elements that are less common or even "exotic" for biomedical purposes have lately made their way into BGs as doping elements to improve their biological and physical characteristics [26, 27]. As third generation biomaterials, BGs can establish a more rapid interfacial link between implants and host tissue than other bio ceramics in the treatment of biological defects [28]. Glass ceramics, which are created by carefully controlling the heat treatment process after crystal nucleation and development inside the glass matrix, contain nano- and/or micro-grained polycrystalline phases embedded in the residual glass phase [29]. These are functional biomaterials recognized for their exceptional performance, adaptable production, and practical designs [30]. Glass ceramics, classified as "bioactive", chemically interact with bone by forming a layer of biologically active apatite in response to the surrounding bodily fluid [31]. When replacing half the amount

of CaO by SrO, the dissolution of $50P_2O_5$-$10Na_2O_{-(40-x)}CaO_{-x}SrO$ glass was minimized [32]. For therapeutic purposes, metal ions can be added to glasses to change their physical or chemical properties. This includes adding Ag, Cu, or Co, for instance, these ions have antibacterial properties [33, 34].

This work research utilized phosphor oxide, strontium carbonate, and calcium carbonate in the glass synthesis. Several characterization techniques, including FTIR, UV-visible spectroscopy, and PL testing, were utilized to study the optical properties of glass. The primary objective was to enhance the performance of the glass material to cater bioactive glasses for biological applications. Therefore, it is important to investigate the impact of Ag doping on this glass composition and determine whether it is possible to obtain Ag-doped strontium-containing phosphate glasses with antimicrobial properties [35].

2. Experimental Work

2.1. Bioactive Glasses Materials

The following materials were used in this study: sodium carbonate (Na_2CO_3) (99.8% purity) (purchased from Shandong Yifengtuo Chemical Co., Ltd.), silver oxide (Ag_2O) (99.8% purity), strontium carbonate ($SrCO_3$) (99.8% purity), and calcium carbonate ($CaCO_3$) (99.8% purity) (purchased from Jinan Future Chemical Co., Ltd.), phosphor oxide (P_2O_5)(99.8% purity)(purchased from Hebei Ruisite Technology Co., Ltd.).

2.2 Phosphate Bioactive Glasses Preparations

The metal-phosphate bio-active glass sample was prepared using weight percentage as follows: First, measured 0.427 wt% of sodium carbonate, 1.5 wt% of phosphorus oxide, 0.75 wt% of strontium carbonate, 3.008 wt% of calcium carbonate, and 0, 0.25, 0.5, and 0.75 wt% of Ag_2O. These ingredients were mixed using a mortar and pestle. The resultant material was poured into a mold that measured 2 cm in diameter and 0.5 cm in height. The mixture was compacted in a hydraulic press at 1000 psi (0.000445Ton) for 15 minutes. The mold was then sintered for 2 hs at 780°C (experimentally by trying) in a furnace. The mold was let to cool to ambient temperature after the sintering process, and the glass was gently removed. These procedures were carried out in order to have the sample of metal-phosphate bio-active glass ready for testing. In this paper, we did not test any transition metal oxides, only Ag_2O. Bioactive materials have an ability to produce a bind to the bone and its ability to develop of new tissue and resorption material [36]. Bioactive glass induces a certain biological reaction in order to produce a connection between the tissues and the material. BGs can establish a rapid interfacial link between BGs and skin tissue. As the Ag_2O is a glass network modifier with its important biological properties, as well as, its antibacterial and anticancer characteristics, researchers interest focused on antibacterial properties of Ag_2O [37].

2.3. Characterization

The FTIR spectra of the prepared phosphate bioactive glasses in powder form were obtained at room temperature using an IR spectrometer (the Bruker Vertex 8V model from Germany). The spectra were recorded within the wavenumber range of 400-4000 cm^{-1}. The measurements were performed with a resolution of 4 cm^{-1} for the phosphate glasses before and after doping with silver oxide. The UV-visible absorption spectra were obtained for polished samples of equal thickness (2mm±0.1 mm) in the undoped and Ag-doped forms. The measurements were conducted in 200-1200 nm range using a spectrophotometer (Shimadzu 3600 recording spectrophotometer, from

Japan). The measurements were repeated to ensure accuracy in determining the positions of the peaks. A spectrofluorometer (Horiba Jobin Yvon Fluorolog) equipped with a sensitive detector was used for the photoluminescence (PL) test. It allows for the excitation of a material with light of specific wavelengths (300-900nm), and then detects and analyzes the emitted light spectrum to provide insights into the material's photoluminescent properties. It enables the gathering of precise and reliable data, shedding light on the intricate relationship between silver oxide concentration and the optical behavior of bioactive phosphate glasses. This information holds significant importance in understanding the potential applications of PBGs in various optical and biomedical fields, such as bioimaging, biosensing, and drug delivery systems.

3. Results and Discussion

3.1. FTIR Analysis

In FTIR spectroscopy, infrared light transmission or absorption of a sample as a function of wavelength or frequency is measured [38]. The sample converts radiation into vibration or rotation. The detector normally produces a signal with a spectrum between 4000 and 400 cm^{-1} [39]. The resulting spectrum can provide information about the functional groups and chemical bonds present in the sample, which can be used to identify the sample or to investigate its properties. The functional groups of the powdered samples, undoped and doped with varying Ag_2O dopant concentrations of (0, 0.25, 0.5 and 0.75g), sintered at 780 °C for 1hr are shown in Figs. 1, 2, 3 and 4, as evaluated using FTIR. The specific peaks observed in the FTIR spectrum of a sample depend on the chemical composition and structure of the material and the particular conditions of the sintering process. Ag_2O can significantly alter the FTIR spectrum of a substance. Ag_2O exhibits distinctive vibrational modes in the infrared range, and the exact locations and intensities of these modes vary with Ag_2O concentration. Therefore, it is possible to detect variations in the vibrational modes associated with Ag-O bonds and learn more about the structure and composition of the material by evaluating its FTIR spectra related to the different amounts of Ag_2O doping. The quantity of Ag_2O in a material also impacts the FTIR peaks intensity. As the Ag_2O concentration rises, more Ag-O bonds are present in the sample, causing the Ag-O vibrational mode peaks to be of larger intensity. The presence of Ag_2O may also impact the intensity of other vibrational modes in the FTIR spectrum depending on the precise chemical environment and interactions between various atoms or functional groups in the material. Therefore, a thorough examination of the entire FTIR spectrum is required to fully comprehend how Ag_2O affects the intensity of various peaks. Here are some potential vibrational modes and related FTIR peaks based on the mixture's chemical composition (P_2O_5, CaO, SrO, Na_2O, and Ag_2O) [40, 41]:

- P-O stretching vibrations: typically occur at around 1200-1000 cm^{-1}.
- Ca-O stretching vibrations: typically occur at around 900-700 cm^{-1}.
- Sr-O stretching vibrations: typically occur at around 650-500 cm^{-1}.
- Na-O stretching vibrations: typically occur at around 1100-900 cm^{-1}.
- Ag-O stretching vibrations: depending on the chemical form of Ag_2O in the mixture, may occur at around 600-400 cm^{-1}.

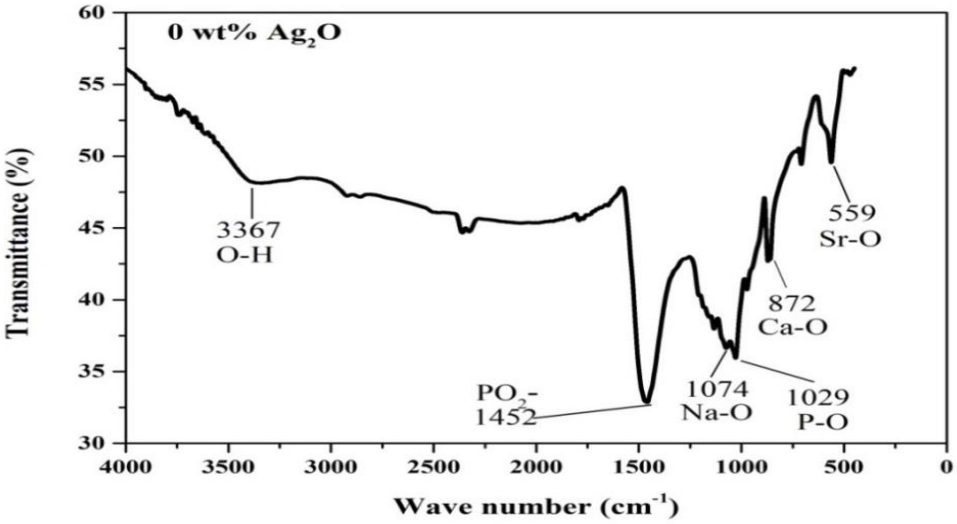

Figure 1: FTIR analysis of calcium phosphate ceramic.

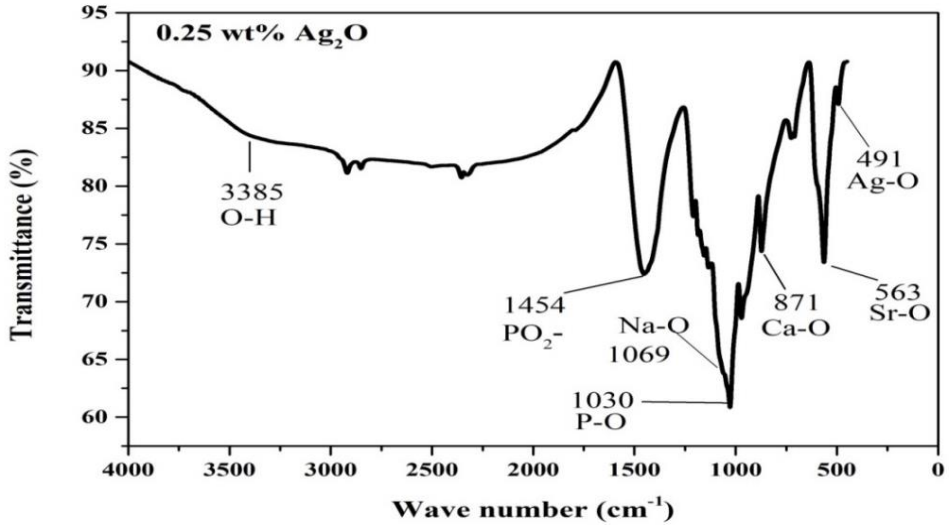

Figure 2: FTIR analysis of calcium phosphate ceramic with 0.25 wt.% Ag_2O.

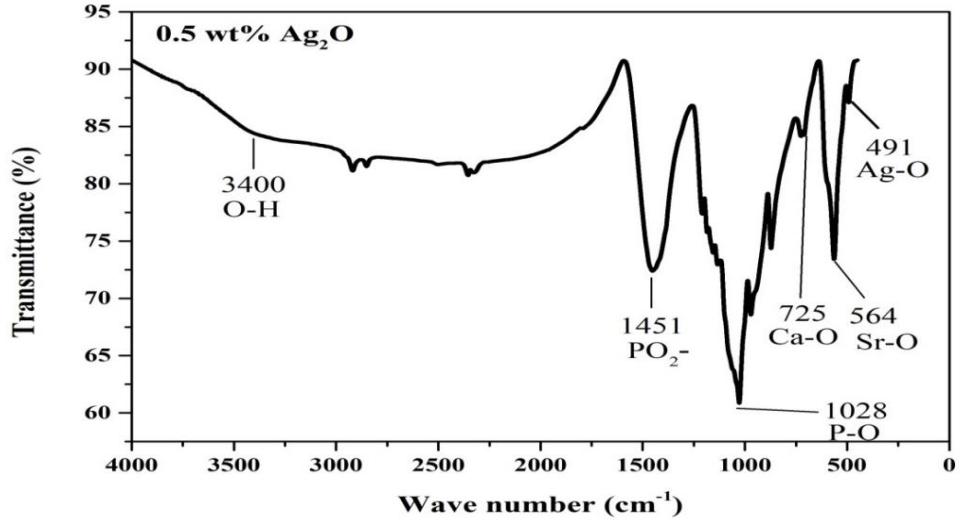

Figure 3: FTIR analysis of calcium phosphate ceramic with 0. 5 wt.% Ag_2O.

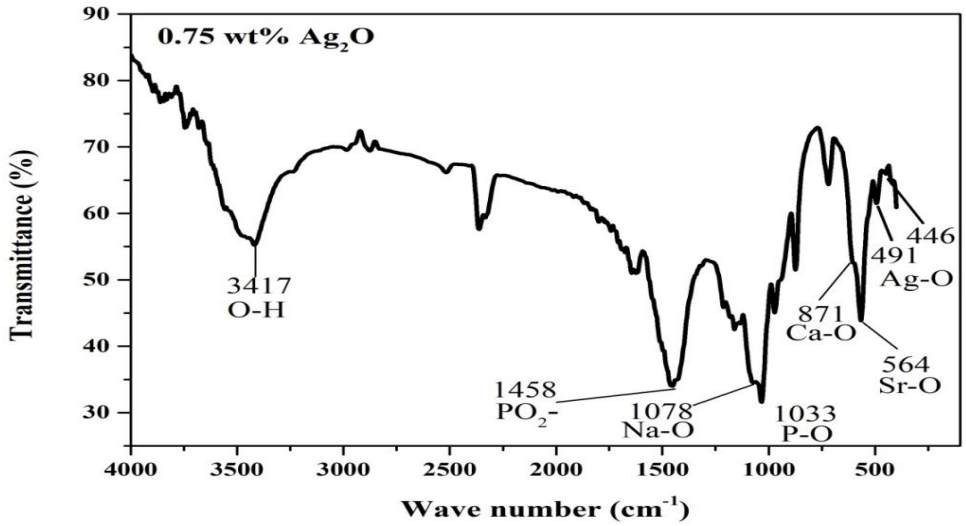

Figure 4: FTIR analysis of calcium phosphate ceramic with 0.75 wt.% Ag_2O.

3.2. Ultraviolet–Visible Spectroscopy

UV-Vis spectrophotometry can assess the optical properties of BAG samples (P_2O_5, CaO, SrO, and Na_2O) doped with Ag_2O at various percentage concentrations (0, 0.25, 0.5, and 0.75%). It measures glass transparency or opacity in the UV spectrum, it can also study the samples with varied concentrations (0, 0.25, 0.5, and 0.75%) of Ag_2O which is used as a solution. This information is essential for material development and optimization. For UV-Vis spectrum analysis, the samples were prepared as powder and used as a suspension in distilled water, which were used as a reference for all Ag_2O phosphate glass compositions. Each sample was tested twice for each concentration and the same result was obtained. Fig. 5 shows the UV-visible absorption spectra of PBGs with different concentrations of Ag_2O. The UV-Vis spectrum showed a shifting toward higher wavelengths with increasing the Ag_2O concentration from 192 nm at 0.5 wt% to 194 nm at 0.75 wt%. Ag_2O, which absorbs strongly in the UV, may activate electrons in its valence band, causing the spectrum peak. The broad UV absorption band of phosphorous oxide (P_2O_5) may overlap with Ag_2O. The shift in the peak from 192 to 194 nm when the concentration of Ag_2O was increased suggests that the absorption at 194 nm is indeed due to the presence of Ag_2O in the composite material. As the concentration of Ag_2O was decreased, there were fewer Ag_2O molecules present to absorb the light at 194 nm, and as a result, the absorption peak shifted slightly to a lower wavelength. The other components in the composite material, such as P_2O_5, CaO, SrO, and Na_2O, could contribute to the overall UV-Vis spectrum and potentially affect the observed shift in the peak. The broad UV absorption band of P_2O_5 may overlap with Ag_2O. However, without specific details about the electronic structure of Ag_2O in the context of phosphate glass, it is challenging to pinpoint the exact nature of the transition. The electronic structure and absorption spectra are influenced by factors, such as the local environment, crystal field effects, and the presence of other elements or impurities in the glass. While metallic silver creates peaks in the visible spectrum, silver ions exhibit absorption in the ultraviolet portion of the UV-Vis spectrum. The absorption peaks at roughly 194 and 192 nm are due to the electronic transitions of Ag+ ions. In Ag_2O, Ag+ ions have a 4d10 electron configuration, corresponding to a filled d orbital. When the Ag+ ion absorbs light energy, one electron from the 4d orbital is excited to the 5s orbital, leading to a 4d10 to 4d9 5s1 transition. The energy required for this transition corresponds to a wavelength of around 194 nm. Therefore, it is reasonable to attribute the absorption peak at around 194 and 192 nm to the 4d10 to 4d9 5s1 transition of Ag+ ions in the sample. It is worth noting that the exact position of the

absorption peak depends on many factors, such as the concentration of Ag+ ions, the crystal field environment, and the presence of other ions in the sample; it also depends on the specific electronic transitions and the local environment of the silver ions. In general, silver particles or clusters with a small number of atoms can exhibit size-dependent electronic properties due to the quantum confinement effects. As the size of the silver nanoparticle or cluster decreases, the energy levels of the electrons become quantized, which can lead to discrete electronic transitions and unique optical properties. For example, Ag_2O clusters have been reported to exhibit electronic transitions in the UV-Vis region, including an absorption peak around 210 nm, which has been attributed to a transition from the HOMO (highest occupied molecular orbital) to the LUMO (lowest unoccupied molecular orbital) of the Ag_2 cluster. Similarly, Ag4 clusters have also been reported to exhibit UV-Vis absorption peaks in the range of 200-250 nm, attributed to electronic transitions between the highest occupied and lowest unoccupied molecular orbitals of the Ag4 cluster [42].

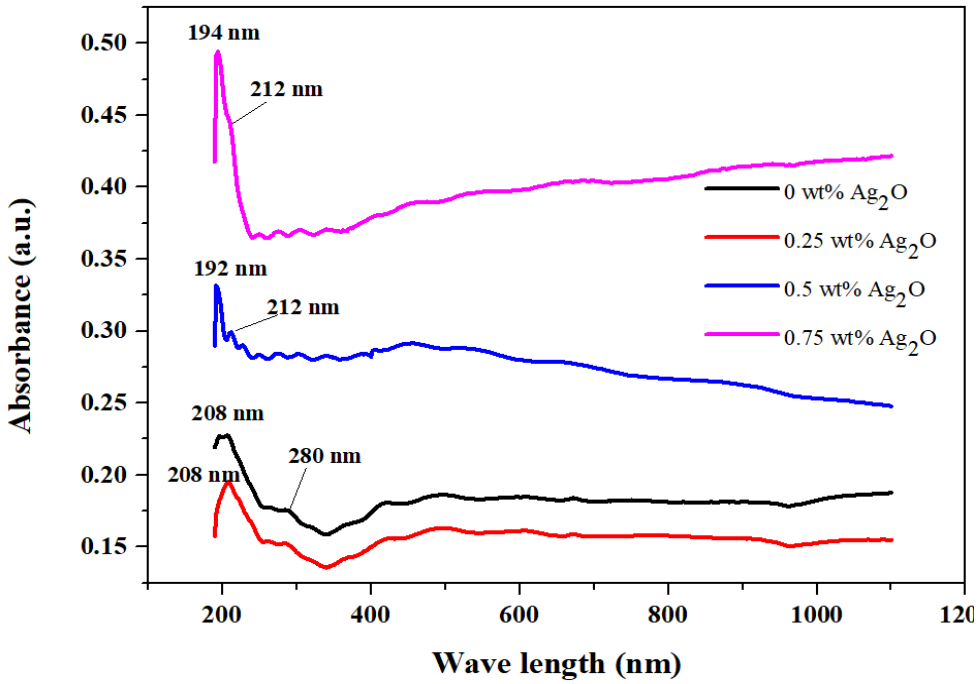

Figure 5: The UV-visible absorption spectra of glass ceramics doped with different concentrations of Ag_2O and calcined at 780°C. The absorption spectra are plotted as a function of wavelength and show the degree of absorption of the sample at different wavelengths.

3.3. Photoluminescent Properties

Photoluminescence (PL) is divided into two classes: fluorescence and phosphorescence. The peaks observed in a PL spectrum are related to the optical properties of the glass, which are influenced by the concentration of Ag_2O. For PL, the excitation/emission slit was used with 10 µm slit width band pass. The addition of Ag_2O to the metal-phosphate bioactive glass can potentially affect the band gap of the glass. The band gap refers to the energy difference between the valence band and the conduction band in a material. It determines the material's ability to absorb or emit light of different wavelengths. PL was conducted to determine the effect of Ag_2O on the band gap of the phosphate bioactive glass. In this test, the glass sample was excited with light of a specific wavelength, and the emitted light spectrum was analyzed. In general, as shown in Figs. 6-9, the peaks of the PL spectra correspond to the absorption of light by the glass at specific wavelengths. The excitation wave length used in this test was 210

nm depending on the UV -Vis λexi peak. The first sample, with no Ag_2O, showed high intensity peaks at 597, and 827 nm and low intensity peaks at 410.8, 495nm. The second sample, of 0.25 wt% Ag_2O doping showed the highest peak at 488.8nm, and several slight intensities at 560, 630 and 874 nm. The third sample, of 0.5 wt% Ag_2O doping manifested very definite sharp peaks with higher intensity than those of the second sample at 379, 508, 611, 708, and 869 nm. The fourth sample, of 0.75 wt% Ag2O doping revealed distinctive peaks at 405.6, 534, 644 and 790 nm. The change in the peak's wavelength is likely due to the interaction between the Ag_2O and the other components of the glass. The concentration of Ag_2O affects the glass structure and properties, which in turn affects its optical properties. The specific wavelengths of the peaks can provide information about the glass's composition and structure, which can be useful for understanding its properties and potential applications [43, 44]. The appearance of several peaks in the PL spectra means several band gaps, so the prepared sample can be used in different technical applications depending on the specific band gap energy. To determine the band gap energy of each sample, the peaks wavelengths obtained from the PL spectra were analyzed. The band gap energy [43] was calculated from the following equation:

$$E = \frac{(hc)}{\lambda} \qquad (1)$$

where: E is the band gap energy, h is Planck's constant (6.626 x 10-34 J.s), c is the speed of light (2.998 x 108 m/s), and λ is the wavelength of the peak in meters.

Table 1. The wavelength (nm) and band gap energy (eV) of metal-phosphate bioactive glass samples with varying silver oxide content.

Sample	Ag_2O (g)	Wave length (nm)	E_g (eV)
1	0	410	3.024
		495	2.505
		597	2.077
		825	1.499
2	0.25	420	2.952
		488.8	2.536
		560	2.214
		874	1.418
3	0.5	379	3.271
		542	2.287
		611	2.029
		708	1.751
		869	1.426
4	0.75	405	3.057
		537	2.322
		644	1.925
		790	1.569

The present work previews several energy gaps in PL test for each Ag_2O concentration. Therefore, high or low energies can be chosen according to the applications of the device which promote a wide scope of application according to the PL test. These PL results were compatible with those of other researchers [44-48].

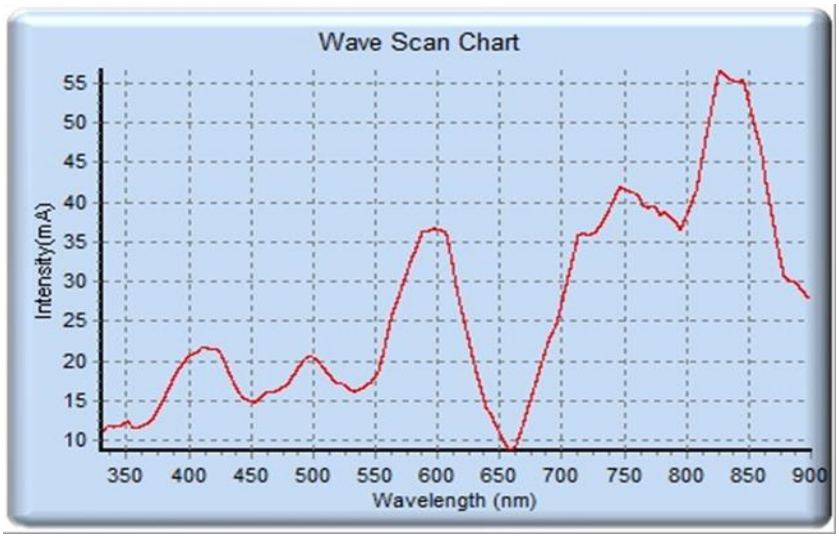

Figure 6: PL spectra of phosphate bioactive glass.

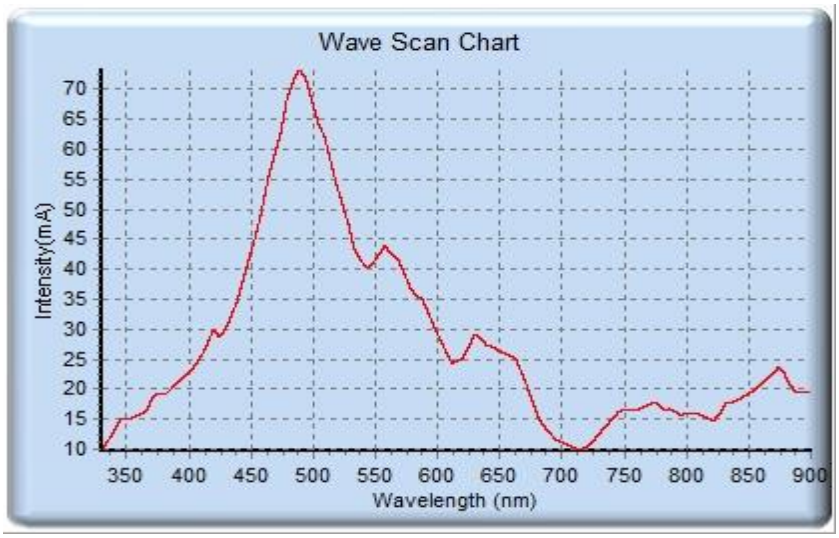

Figure 7: PL spectra of phosphate bioactive glass doped with 0.25 g Ag_2O.

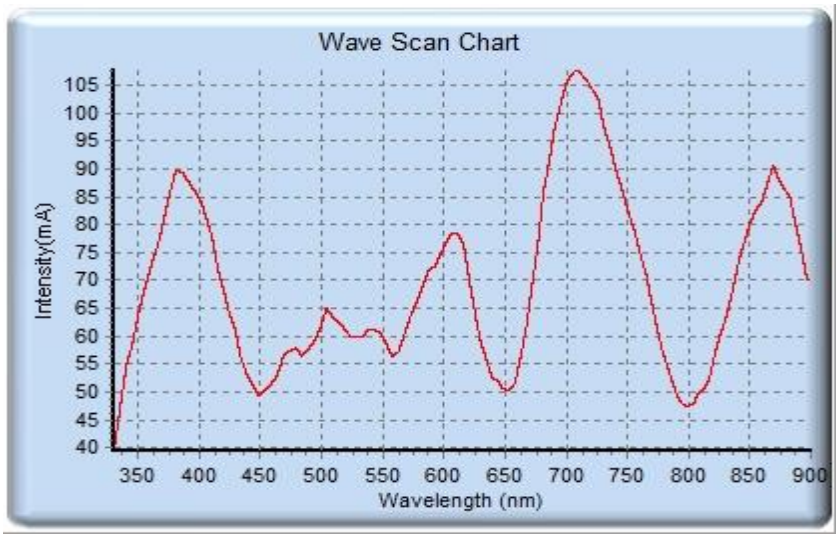

Figure 8: PL spectra of phosphate bioactive glass doped with 0.5 g Ag_2O.

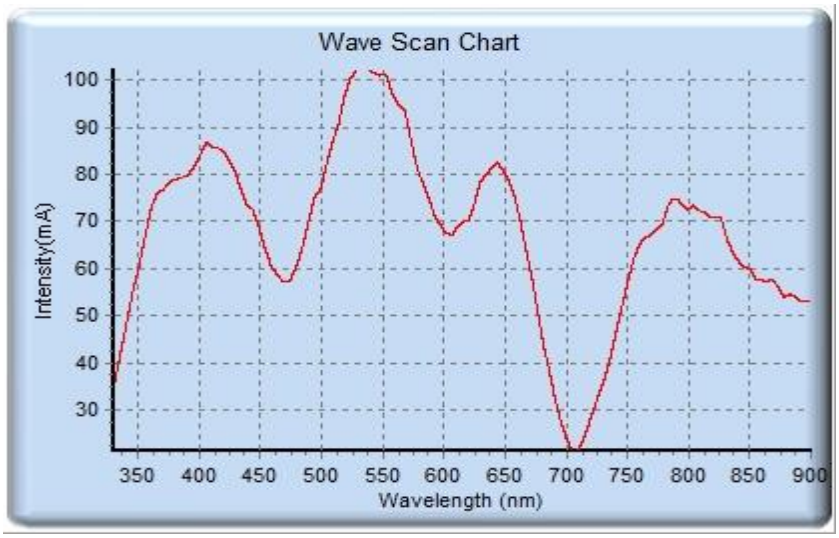

Figure 9: PL spectra of phosphate bioactive glass doped with 0.75 g Ag_2O.

4. Conclusions

This work examined how Ag_2O concentration affects the optical properties of PBGs. PBGs' adjustable chemical resistance and bioactivity make them a prospective medicinal alternative to silicate glasses. FTIR, UV-visible, and PL were used to assess powder samples sintered at 780°C for 2 hrs with and without Ag_2O doping. Related to the FTIR analysis, the vibrational modes and the corresponding peaks attributed to P-O stretching vibrations, Ca-O, Sr-O, Na-O and Ag-O stretching vibrations were observed. The absorption peaks at around 194 and 192 nm were noticed in the UV-Vis spectrum of the prepared samples. When the concentration of Ag_2O was increased, the peak shifted from 192 to 194nm. The other components in the composite material could also contribute to the absorption in the UV-Vis spectrum. Moreover, the exact position of the absorption peak could depend on several factors, such as the concentration of Ag+ ions, the crystal field environment, and the presence of other ions in the sample. Overall, the UV-Vis technique can be used to detect the presence and concentration of Ag_2O and other silver species in bioactive glasses. The PL technique was used to calculate the energy gap. It has been concluded that adding Ag_2O to phosphate glass increased the energy gap, especially at 0.5% Ag_2O concentration. This increase results in a change in some of the material's physical properties, such as an increase in the conductivity of the glass and an increase in motivation.

References

1. D. K. Al-Nasrawy, I. M. Abdulmajeed, F. T. Noori, A. H. Abaid, and K. M. Thajeel, J. Kufa Phys. **3**, 30, (2019).
2. C. Li, C. Wang, A. R. Boccaccini, and K. Zheng, J. Non-Cryst. Sol. X **17**, 100159 (2023).
3. V. A. Gobbo, V. S. Parihar, M. Prato, M. Kellomäki, E. Verne, S. Spriano, and J. Massera, Ceram. Int. **49**, 1261 (2023).
4. A. Elrayah, D. Xiao, E. Suliman, and J. Weng, Ceram. Int. **45**, 18931 (2019).
5. T. A. Kareem and D. K. Mahdi, Eurasian Chem. Commun. **4**, 330 (2022).
6. A. Elrayah, J. Weng, and E. Suliman, 2019 International Conference on Computer, Control, Electrical, and Electronics Engineering (ICCCEEE) (Khartoum, Sudan IEEE, 2019). p. 1.
7. D. S. Brauer, Angewan. Chem. Int. Ed. **54**, 4160 (2015).

8. L. C. A. Da Silva, F. G. Neto, S. S. C. Pimentel, R. Da Silva Palácios, F. Sato, K. M. Retamiro, N. S. Fernandes, C. V. Nakamura, F. Pedrochi, and A. Steimacher, J. Non-Cryst. Sol. **554**, 120611 (2021).
9. S. Naseri, G. Griffanti, W. C. Lepry, V. B. Maisuria, N. Tufenkji, and S. N. Nazhat, J. American Ceram. Soci. **105**, 1711 (2022).
10. A. Rahimnejad Yazdi, L. Torkan, W. Stone, and M. R. Towler, J. Biomed. Mat. Res. B Appl. Biomat. **106**, 367 (2018).
11. C. Bergmann, M. Lindner, W. Zhang, K. Koczur, A. Kirsten, R. Telle, and H. Fischer, J. the European Ceram. Soci. **30**, 2563 (2010).
12. K. A. Cole, G. A. Funk, M. N. Rahaman, and T. E. Mciff, J. Biomed. Mat. Res. B Appl. Biomat. **108**, 2765 (2020).
13. E. A. Abou Neel, D. M. Pickup, S. P. Valappil, R. J. Newport, and J. C. Knowles, J. Mat. Chem. **19**, 690 (2009).
14. C. R. Arciola, D. Campoccia, and L. Montanaro, Nat. Rev. Microbio. **16**, 397 (2018).
15. H. N. Wilkinson, S. Iveson, P. Catherall, and M. J. Hardman, Front. Microbio. **9**, 337311 (2018).
16. V. Dhivya, G. Rajkumar, S. Mahalaxmi, K. Rajkumar, B. S. Karthikeyan, S. Kavitha, R. Karpagam, K. Sakthipandi, and G. Sathishkumar, Ceram. Int. **48**, 25346 (2022).
17. Z. Xu, C. Zhang, X. Wang, and D. Liu, ACS Appl. Bio. Mat. **4**, 3985 (2021).
18. F. M. Aldakheel, M. M. E. Sayed, D. Mohsen, M. H. Fagir, and D. K. El Dein, Gels **9**, 530 (2023).
19. F. Foroutan, B. A. Kyffin, A. Nikolaou, J. Merino-Gutierrez, I. Abrahams, N. Kanwal, J. C. Knowles, A. J. Smith, G. J. Smales, and D. Carta, RSC Advances **13**, 19662 (2023).
20. Z. H. Dhoondia and H. Chakraborty, Nanomat. Nanotech. **2**, 15 (2012).
21. S. Sagadevan, Int. J. Nanoelect. Mat. **9**, 37 (2016).
22. B. Karmakar, *Functional Glasses and Glass-Ceramics:Processing, Properties and Applications*, Butterworth-Heinemann, (2017).
23. J. Massera, S. Fagerlund, L. Hupa, and M. Hupa, J. American Ceram. Soci. **95**, 607 (2012).
24. A. R. Boccaccini, P. X. Ma, and L. Liverani, *Tissue Engineering Using Ceramics and Polymers* (UK, Woodhead Publishing, 2021).
25. F. N. Raja, T. Worthington, L. P. De Souza, S. B. Hanaei, and R. a. J. Martin, ACS Biomat. Sci. Eng. **8**, 1193 (2022).
26. C. Wen, J. Qian, L. Luo, J. Zeng, B. Sa, X. Zhan, J. Wang, L. Sheng, and Y. Zheng, J. Non-Cryst. Sol. **578**, 121329 (2022).
27. E. Cruces, N. Arancibia-Miranda, K. Manquián-Cerda, F. Perreault, N. Bolan, M. I. Azócar, V. Cubillos, J. Montory, M. A. Rubio, and B. Sarkar, ACS Appl. Nano Mat. **5**, 1472 (2022).
28. W. N. Wan Jusoh, K. A. Matori, M. H. Mohd Zaid, N. Zainuddin, M. Z. Ahmad Khiri, N. A. Abdul Rahman, R. Abdul Jalil, and E. Kul, Materials **14**, 954 (2021).
29. D. Williams, Mat. Today **7**, 24 (2004).
30. S. Thomas, P. Balakrishnan, and M. S. Sreekala, *Fundamental biomaterials: ceramics* (US, UK, Woodhead Publishing, 2018).
31. S. M. Rabiee, N. Nazparvar, M. Azizian, D. Vashaee, and L. Tayebi, Ceram. Int. **41**, 7241 (2015).
32. J. Massera, L. Petit, T. Cardinal, J.-J. Videau, M. Hupa, and L. Hupa, J. Mat. Sci. Mat. Med. **24**, 1407 (2013).

33. C. Wu, Y. Zhou, M. Xu, P. Han, L. Chen, J. Chang, and Y. Xiao, Biomaterials **34**, 422 (2013).
34. G. Poongodi, P. Anandan, R. M. Kumar, and R. Jayavel, Spectrochim. Acta A Molec. Biomolec. Spectro. **148**, 237 (2015).
35. R. H. Hussian and D. K. Mahdi, E. European J. Phys. **3**, 321 (2023).
36. L. L. Hench, I. D. Xynos, and J. M. Polak, J. Biomat. Sci. Poly. Ed. **15**, 543 (2004).
37. P. Naresh, N. Narsimlu, C. Srinivas, M. Shareefuddin, and K. S. Kumar, J. Non-Cryst. Sol. **549**, 120361 (2020).
38. A. B. D. Nandiyanto, R. Oktiani, and R. Ragadhita, Indonesian J. Sci. Tech. **4**, 97 (2019).
39. M. Taha, M. Hassan, S. Essa, and Y. Tartor, Int. J. Veterin Sci. Med. **1**, 15 (2013).
40. M. Kuwik, J. Pisarska, and W. A. Pisarski, Materials **13**, 4746 (2020).
41. E. Abdallah, M. Meikhail, A. El-Adawy, H. A. Othman, and A. Abdelghany, J. Bio. Tribo-Corr. **8**, 39 (2022).
42. C. Mariappan and N. Ranga, Ceram. Int. **43**, 2196 (2017).
43. A. L. Stanford and J. M. Tanner, *Physics for Students of Science and Engineering* (New York, Academic Press, 2014).
44. A. S. Rao, J. Ashok, B. Suresh, G. N. Raju, N. Venkatramaiah, V. R. Kumar, I. Kityk, and N. Veeraiah, J. All. Comp. **712**, 672 (2017).
45. V. Prasad, B. Suresh, M. Kostrzewa, Y. Gandhi, A. Ingram, A. S. S. Reddy, V. R. Kumar, and N. Veeraiah, J. Non-Cryst. Sol. **500**, 460 (2018).
46. A. Siva Sesha Reddy, A. Ingram, M. G. Brik, M. Kostrzewa, P. Bragiel, V. Ravi Kumar, and N. Veeraiah, J. American Ceram. Soci. **100**, 4066 (2017).
47. A. S. S. Reddy, M. Brik, J. S. Kumar, M. Graça, G. N. Raju, V. R. Kumar, M. Piasecki, and N. Veeraiah, Ceram. Int. **42**, 17269 (2016).
48. A. S. S. Reddy, M. Kostrzewa, A. Ingram, N. Purnachand, P. Bragiel, V. R. Kumar, I. Kityk, and N. Veeraiah, J. European Ceram. Soci. **38**, 2010 (2018).

دراسة إضافة ثاني اكسيد الفضة على بعض الخواص البصرية لزجاج الفوسفات النشط حيويا

رقية حسن حسين[1] ودنيا كامل مهدي[1]

[1]قسم الفيزياء، كلية العلوم، جامعة بغداد، بغداد، العراق.

الخلاصة

تبحث هذه الدراسة في تأثير تركيز أكسيد الفضة (Ag_2O) على الخصائص البصرية لنظارات الفوسفات النشطة بيولوجيًا (PBGs). ظهرت PBGs كبدائل واعدة لزجاج السيليكات التقليدي في المجال الطبي بسبب نشاطها الحيوي الممتاز ومقاومتها الكيميائية. تم تلبيد عينات المسحوق بتراكيز Ag_2O المتغيرة (0، 0.25، 0.5، و0.75 غرام) عند 780 درجة مئوية لمدة ساعة واحدة. تم إخضاع العينات لاختبارات FTIR وUV-Vis الطيفي واختبارات اللمعان الضوئي (PL) لتقييم مجموعاتها الوظيفية وخصائصها البصرية من خلال تحليل طيف FTIR للمواد التي تحتوي على كميات مختلفة من Ag_2O، من الممكن تحديد التغييرات في أوضاع الاهتزاز المرتبطة بروابط Ag-O، والحصول على نظرة ثاقبة حول بنية المادة وتكوينها، فقد أدى إدخال Ag_2O إلى تغيير طيف FTIR. مع زيادة تركيز Ag_2O، تم تعزيز أوضاع اهتزاز Ag-O، مما يشير إلى المزيد من روابط Ag-O. قام التحليل الطيفي للأشعة المرئية وفوق البنفسجية بتقييم الخصائص البصرية للأشعة فوق البنفسجية. أثرت قمم امتصاص Ag_2O عند 194 و192 نانومتر على الخصائص البصرية للعينات. مع زيادة تركيز Ag_2O، تحول موقع الذروة من 192 نانومتر إلى 194 نانومتر، مما يؤكد هذه العلاقة. قد تمتص مكونات أخرى مثل P_2O_5 أيضًا الأشعة فوق البنفسجية، كما فحصت اختبارات PL أيضًا كيفية تأثير تركيز Ag_2O على الخصائص البصرية للزجاج المعدني الفوسفاتي وطاقة فجوة النطاق. كشفت قمم أطياف PL وطاقات فجوة النطاق أن Ag_2O قد غير التركيب الكهربائي للزجاج ونشاطه البصري. تساعد هذه الاكتشافات في تحسين الزجاج المعدني ثنائي الفوسفات من أجل الغرسات الطبية الحيوية والطلاءات التي تحجب الأشعة فوق البنفسجية.

الكلمات المفتاحية: زجاج الفوسفات النشط بيولوجيًا (PBG)، زجاج السيليكات، ثنائي فوسفات الكالسيوم، تحويلات فورير للاشعة الحمراء (FTIR)، كربونات السترونتيوم ($SrCO_3$).